Published in final edited form as:

Nat Immunol. 2014 October ; 15(10): 920–928. doi:10.1038/ni.2986.

Diversification of TAM receptor function

Anna Zagórska[1], **Paqui G. Través**[1], **Erin D. Lew**[1], **Ian Dransfield**[2], and **Greg Lemke**[1,3]

[1]Molecular Neurobiology Laboratory, The Salk Institute for Biological Studies, La Jolla, CA 92037

[2]MRC Centre for Inflammation Research, University of Edinburgh, Edinburgh EH16 4TJ, United Kingdom

[3]Immunobiology and Microbial Pathogenesis Laboratory, The Salk Institute for Biological Studies, La Jolla, CA 92037

Abstract

Apoptotic cell clearance is critical for both tissue homeostasis and the resolution of inflammation. We found that the TAM receptor tyrosine kinases Axl and Mer played distinct roles as phagocytic receptors in these two settings, where they exhibited divergent expression, regulation, and activity. Mer acted as a tolerogenic receptor in resting macrophages and in settings of immune suppression. Conversely, Axl was an inflammatory response receptor whose expression was induced by pro-inflammatory stimuli. Axl and Mer displayed distinct ligand specificities, ligand-receptor complex formation in tissues, and receptor shedding upon activation. These differences notwithstanding, phagocytosis by either protein was strictly dependent on receptor activation that was triggered by bridging TAM receptor–ligand complexes to the ‘eat-me’ signal phosphatidylserine on apoptotic cell surfaces.

Keywords

Axl; Mer; GAS-6; Protein S; macrophage; phagocytosis; apoptosis

INTRODUCTION

Billions of apoptotic cells are generated each day in the body’s tissues, and the rapid clearance of these dead cells is essential for both tissue homeostasis and resolution of the inflammatory response to infection. Inefficient clearance can lead to tissue damage and the development of autoimmunity[1]. However, the mechanisms responsible for apoptotic cell

Correspondence should be addressed to: Greg Lemke, MNL-L, The Salk Institute, 10010 N. Torrey Pines Rd., La Jolla, CA 92037, Tel 858-453-4100 ext 1542, Fax 858-455-6138, lemke@salk.edu.

AUTHOR CONTRIBUTIONS

A.Z. designed and performed the experiments; P.G.T. aided in the design and execution of *in vivo* experiments; E.D.L. prepared purified recombinant GAS-6; I.D. aided in the design of the flow cytometry-based phagocytosis assay; G.L. contributed to the design of the experiments and wrote the manuscript.

COMPETING FINANCIAL INTERESTS

G.L. is a shareholder in Kolltan Pharmaceuticals.

clearance in inflammatory versus homeostatic settings are unknown. We sought to determine whether individual members of the TAM family of receptor tyrosine kinases (RTKs) – TYRO3, Axl and Mer[2] – might be specialized to function in these very different environments.

The TAM RTKs regulate the innate immune response[3–5], mediate the homeostatic phagocytosis of apoptotic cells and membranes in adult tissues[6–9], facilitate the infection of target cells by enveloped viruses[10,11], and contribute to the progression and metastasis of human cancers[12–14]. These diverse activities notwithstanding, the specific roles played by individual TAM receptors, together with their ligands GAS-6 and Protein S, are poorly understood.

Genetic studies have shown that TAM signaling plays an especially important role in sentinel cells of the immune system[3,4], where the principal TAM receptors are Axl and Mer. Activation of either Mer or Axl in these cells has been found to dampen immune activation[3], and Axl upregulation and activation in dendritic cells (DCs) is an intrinsic negative feedback inhibitor of the innate immune response[5,15]. Accordingly, deficiencies in TAM signaling result in profound autoimmunity[3,4].

We found that Axl and Mer are dedicated to function in inflammatory and tolerogenic settings, respectively. Macrophage expression of Mer was upregulated by immunosuppressive agents, such as dexamethasone, whereas Axl was inhibited by these agents. Conversely, pro-inflammatory agents upregulated expression of Axl and inhibited expression of Mer. We showed that Mer and Axl specifically mediated the phagocytosis of apoptotic cells in homeostatic and inflammatory environments, respectively, and that catalytic activation of the receptors was required for these events. Importantly, this activation must be induced by a TAM ligand whose binding bridges a phagocyte TAM receptor to the ‘eat-me’ signal phosphatidylserine (PtdSer) on the target apoptotic cell.

We further demonstrated an all-or-none difference in ligand dependence between Mer and Axl – both GAS-6 and Protein S drove Mer-dependent phagocytosis, but only GAS-6 was capable of driving Axl-dependent phagocytosis. GAS-6 was constitutively pre-bound to Axl in tissues *in vivo* without significant activation of the receptor, and the presence of GAS-6 in these tissues was dependent on the co-expression of Axl but independent of Mer and TYRO3. Finally, activation-induced proteolytic cleavage of the Axl extracellular domain liberated Axl-GAS-6 complexes, resulting in the rapid removal of both receptor and ligand from tissues. These features of TAM biology must be taken into account in the design and application of any TAM-targeted therapy.

RESULTS

Differential expression of Axl and Mer

We analyzed TAM expression in both bone marrow-derived macrophages (BMDMs) and dendritic cells (BMDCs) *in vitro*, and in immune cell subsets *in vivo*. In BMDCs, prepared using the growth factor GM-CSF[16], Axl was far more prominently expressed than Mer (Fig. 1a). These cultures also expressed a low amount of TYRO3. In contrast, BMDMs expressed

abundant Mer, minimal Axl, and no TYRO3 (Fig. 1a). Tyrosine autophosphorylation of Mer was stimulated by both Protein S and GAS-6, but Axl could only be activated by GAS-6 (Fig. 1b).

In vivo, we observed several tissues in which Axl and Mer exhibited expression patterns that paralleled those of cultured macrophages and DCs. For example, in the spleen, $CD68^+$ tingible body macrophages were primarily Mer^+ (Supplementary Fig. 1)[17], whereas $CD11c^+$ white pulp DCs were mostly Axl^+[18]. Conversely, we found that $CD11c^+CD11b^-MHCII^-$ cells in the lung expressed abundant Axl but low amounts of Mer (Supplementary Fig. 1). At the same time, we observed some populations – such as red pulp macrophages in the spleen and Kupffer cells in the liver – in which Axl and Mer were co-expressed (Supplementary Fig. 1). Finally, we detected divergent expression of Mer and Axl within BMDM cultures: individual BMDM cells expressed either Mer or Axl, but not both (Supplementary Fig. 2a, upper row).

Mer is induced by tolerogenic stimuli

The differential expression of Axl and Mer in macrophages and DCs was matched by reciprocal responses to tolerogenic stimuli. The immunosuppressive glucocorticoid dexamethasone (Dex) has been shown to upregulate expression of Mer in human monocyte-derived macrophages[19], and we found that this was also true for mouse BMDMs (Fig. 1c and Supplementary Fig. 2b). The time course of Dex-mediated upregulation of Mer protein and mRNA (Fig. 1c,d, respectively) was inversely correlated with Dex-mediated downregulation of Axl protein and mRNA (Fig. 1c,d, respectively, and Supplementary Fig. 2c). Since other nuclear hormones have been reported to upregulate macrophage expression of Mer[20,21], we tested three other nuclear hormone receptor agonists – the LXR agonist T0901317, the PPARδ agonist GW501516, and the PPARγ agonist BRL49653. Of these, only the LXR agonist potentiated Mer expression (Fig. 1e). Although lipopolysaccharide (LPS) was a potent inducer of Axl in BMDMs (Fig. 1e), co-incubation with Dex suppressed this effect. Dex-mediated induction of Mer and suppression of Axl occurred at the mRNA level (Fig. 1f). In addition to Dex, the related corticosteroids hydrocortisone and aldosterone also induced Mer in BMDMs (Supplementary Fig. 3).

Glucocorticoid immunosuppression is marked by changes in macrophage gene expression and the inhibition of MAPK signaling pathways[22]. Since we found that *Mer* upregulation in response to Dex was faster than the induction of canonical Dex targets such as *Fpr1* or *Mrc1* (Supplementary Fig. 4a), we asked whether any of these Dex effects might depend on upregulation of Mer or downregulation of Axl. We found that Dex-mediated inhibition of LPS-induced tumor necrosis factor (TNF) (Supplementary Fig. 4b), Dex-mediated changes in gene expression (Supplementary Fig. 4c), and Dex inhibition of MAPK and Akt signaling (Supplementary Fig. 4d) were all Axl- and Mer-independent.

Axl is induced by inflammatory stimuli

Polarization of macrophages into a ‘classically activated’ M1 phenotype is stimulated by Toll-like receptor (TLR) ligands and interferon-γ (IFN-γ), an ‘alternatively activated’ M2 phenotype by interleukin 4 (IL-4) and IL-13, and a ‘regulatory-tolerogenic’ phenotype by

anti-inflammatory agents[23]. We found that BMDM expression of Axl was potently stimulated by inflammatory mediators of classical M1 activation, which in general had modest inhibitory effects on Mer expression. LPS, for example, elevated *Axl* mRNA with a time course that followed the induction of inducible nitric oxide synthetase (*Nos2*) mRNA (Fig. 2a). Over the same time course, expression of *Gas6* and *Pros1* mRNA was modestly reduced (Fig. 2a), as noted previously[24].

We surveyed a panel of pattern recognition receptor ligands for their ability to regulate Axl and Mer expression in BMDMs (Fig. 2b). Axl expression was elevated by many of these inflammatory mediators, the most potent of which were ligands for TLR3, TLR4, and RIG-I, such as LPS and poly(I:C) (Fig. 2b,c). TNF and IFN-α also elevated Axl expression (Fig. 2c). TLR ligands induce Axl expression in DCs via type I IFNs, as IFN receptor-deficient DCs fail to up-regulate Axl in response to poly(I:C)[5]. Accordingly, we found that IFN-α upregulation of Axl in BMDMs was slightly faster than its up-regulation by poly(I:C) (Supplementary Fig. 5). IFN-γ potently induced both Axl and Mer (Fig. 2c). However, individual BMDM cells in IFN-γ-treated cultures were again either Mer^+ or Axl^+: only a small minority of these cells co-expressed both receptors (Supplementary Fig. 2a, bottom row).

While these results are consistent with Axl being a marker of M1 activation, we found that IL-4 also elevated Axl and inhibited Mer expression in BMDMs (Fig. 2d). As expected, these reciprocal changes in receptor expression were paralleled by reciprocal changes in Mer and Axl autophosphorylation in response to recombinant GAS-6 (Fig. 2d). Using surface biotinylation, we verified that Dex-mediated stimulation of Mer and LPS-mediated stimulation of Axl were both associated with increased expression of these receptors on the cell surface (Fig. 2e). Together, the above observations indicate that Axl and Mer display divergent profiles of expression and regulation in inflammatory versus tolerogenic settings, respectively. In general, the induction of Mer expression is accompanied by the inhibition of Axl, and vice versa.

TAM specialization during phagocytosis

Genetic analyses have shown that Mer is required for the phagocytosis of apoptotic cells in multiple tissues[2,6,7,9,25], but the possible role of Axl in that process has been less well studied[18,26]. We first examined the mobilization of Axl and Mer to the surface of BMDMs in contact with apoptotic thymocytes. We labeled these apoptotic cells with a cytoplasmic dye (orange cell tracker) and incubated them with BMDMs for 30 min. In the absence of a TAM ligand, neither Axl nor Mer were localized to the site of BMDM association with the apoptotic cell (Fig. 3a,b, left). However, upon addition of either GAS-6 or Protein S to Mer^+ BMDMs - or of GAS-6 but not Protein S to Axl^+ BMDMs - we observed a striking relocalization of Mer and Axl to the membrane surrounding entrapped apoptotic cells (Fig. 3a–c). Poly(I:C)-treated Axl^+ BMDMs formed a readily apparent phagocytic cup during the engulfment of apoptotic cells, as visualized by scanning electron microscopy (Fig. 3d).

To assess quantitatively the ability of Axl to mediate apoptotic cell phagocytosis, we used wild-type, $Axl^{-/-}$ and $Mertk^{-/-}$ macrophages in a flow cytometry-based phagocytosis assay that exploits pHrodo[27], a pH-sensitive fluorescent dye (**Methods** and Supplementary Fig. 6).

We performed these experiments in untreated BMDM cultures, and in cultures treated with Dex, poly(I:C) or IFN-γ. We found that untreated (Mer-expressing) BMDMs had a modest phagocytic index that was stimulated by both GAS-6 and Protein S, and that apoptotic cell phagocytosis was Mer-dependent and Axl-independent (Fig. 3e). Those responses were significantly enhanced in Dex-treated cells (Fig. 3f). In marked contrast, phagocytosis by poly(I:C) treated, Axl-expressing BMDMs could only be stimulated by GAS-6, and this phagocytosis was entirely Axl-dependent (Fig. 3g). IFN-γ-treated BMDM cultures contained cells that highly expressed either Axl or Mer (Supplementary Fig. 2a, bottom). Phagocytic activity in these cultures also was potentiated by GAS-6, but this potentiation was completely absent only in *Axl*$^{-/-}$*Mertk*$^{-/-}$ cultures (Fig. 3i). Together, these results demonstrate that both Axl and Mer function as phagocytic receptors *in vitro*, but that they act in divergent settings and rely on different ligands.

Basal phagocytosis was decreased in Dex-treated cells and elevated in poly(I:C)-treated cells, and neither of these effects was TAM-dependent (Fig. 3f,g). We therefore measured changes in mRNAs encoding other known mediators of apoptotic cell recognition and engulfment in response to both pro- and anti-inflammatory stimuli. We found that many of these were co-regulated with either Axl or Mer. For example, mRNA encoding the C-type lectin LOX-1 (ref. [28]) was co-regulated with Axl (Fig. 3h), whereas mRNA encoding the PtdSer receptor BAI1 (ref. [29]) was co-regulated with Mer (Fig. 3h). These results indicate that activated and tolerogenic macrophage populations use distinct cohorts of phagocytic mediators to recognize and engulf apoptotic cells.

To assess the ability of Axl to mediate the phagocytosis of apoptotic cells by macrophages *in vivo*, we intraperitoneally administered pHrodo-labeled apoptotic cells 16 h after a poly(I:C) injection, and allowed 1 h for phagocytosis prior to the isolation of peritoneal macrophages. CD11b^{+} peritoneal macrophages expressed high amounts of Axl in response to poly(I:C) injection (Fig. 3j). We found that *Axl*$^{-/-}$ poly(I:C)-treated macrophages less efficiently phagocytized apoptotic cells (Fig. 3k).

We also assayed the potential role of TYRO3 in apoptotic cell phagocytosis by BMDCs. BMDCs expressed minimal TYRO3 and this expression was further downregulated by proinflammatory stimuli. Regulation and activation of Axl and Mer in BMDCs paralleled that observed for BMDMs (Supplementary Fig. 7a,b). Using BMDCs from *Tyro3*$^{-/-}$ mice, we found that TYRO3 was not required for Dex-induced Mer-dependent or for poly(I:C)-induced Axl-dependent phagocytosis of apoptotic cells (Supplementary Fig. 7c,d). The minimal TYRO3 expressed by BMDCs therefore does not play a significant role in apoptotic cell phagocytosis.

TAM activity during phagocytosis

We assessed the ability of apoptotic cells, in concert with TAM ligands, to modulate TAM receptor kinase activity in BMDMs. GAS-6 and Protein S are produced by BMDMs (Fig. 1e), and culture medium supplemented with 10% serum contains ~30 nM Protein S. Addition of apoptotic cells to BMDMs for 30 min potentiated autophosphorylation of Axl and, to a greater extent, Mer (Fig. 4a, lanes 1 and 2). Dex-treated cells exhibited more Mer kinase activity, which was further elevated by apoptotic cell addition, whereas no Axl

activity was detectable (Fig. 4a, lanes 3 and 4). Conversely, LPS-treated BMDMs exhibited enhanced autophosphorylation of Axl upon exposure to apoptotic cells, but no activation of Mer (Fig. 4a, lanes 5 and 6).

To control ligand concentrations in this assay, we cultured untreated BMDMs overnight in serum-free medium, and washed the cells extensively prior to the assay. We then added low concentrations of purified ligands, 2 nM GAS-6 or 10 nM Protein S, with and without the addition of apoptotic cells, and assayed Mer and Axl autophosphorylation. Without added GAS-6 or Protein S, the presence of apoptotic cells alone had no effect on the basal kinase activity of either Mer or Axl (Fig. 4b, lanes 1 and 2). Addition of GAS-6 resulted in an increase in Mer and, to lesser extent, Axl phosphorylation, consistent with the fact that these cultures express much more Mer than Axl (Fig. 4b, lane 3). GAS-6 activation of Mer and Axl was significantly enhanced by the inclusion of apoptotic cells (Fig. 4b, lane 4). Protein S likewise stimulated Mer autophosphorylation, which was also enhanced by the inclusion of apoptotic cells, but had no effect on Axl (Fig. 4b, lanes 5 and 6).

To determine if tyrosine kinase activity of the TAM receptors is required for apoptotic cell phagocytosis, we used BMS-777607, a small molecule inhibitor of the Met, Ron, and TAM RTKs[30]. We have previously shown that this compound efficiently inhibits GAS-6-driven activation of both Mer and Axl in BMDCs[10]. We observed the same degree of TAM inhibition in BMDMs (Fig. 4c). When we added BMS-777607 to BMDMs grown under basal conditions, or in the presence of Dex or poly(I:C), we found that BMS-777607 blocked phagocytosis in all settings (Fig. 4d). Thus, Axl and Mer tyrosine kinase activities are both induced and required for TAM-dependent apoptotic cell phagocytosis.

Axl-dependent GAS-6 expression *in vivo*

We observed that the maintenance of GAS-6 in many tissues was entirely dependent upon simultaneous expression of Axl. In sections of spleen, small intestine, liver, and lung, where GAS-6 was readily detected by immunohistochemistry in wild-type mice, its expression was lost in *Axl*$^{-/-}$ mutants (Fig. 5a). This effect was specific to Axl, as GAS-6 presence was unaltered in these tissues in *Mertk*$^{-/-}$ (Fig. 5a) and *Tyro3*$^{-/-}$ (data not shown) mice. Immunoblots of splenic lysates for GAS-6 confirmed the *in vivo* immunostaining (Fig. 5b). Consistent with the hypothesis that most or all of splenic GAS-6 is normally bound to Axl, we found that the basal Axl phosphorylation was slightly elevated relative to that seen in *Gas6*$^{-/-}$ splenic lysates (Fig. 5c), but this basal Axl activation was still far below that observed upon addition of GAS-6 *in vitro.*

When we co-stained sections of splenic red pulp with Axl and GAS-6 antibodies, we observed perfect co-localization (Fig. 5d). Similarly, when we stained poly(I:C)-treated BMDM cultures we found that BMDMs displaying surface Axl were always the same cells that displayed surface GAS-6, and vice versa (Fig. 5e). Specific steady state binding of GAS-6 to Axl may account for higher basal activation of Axl than Mer (e.g., Fig. 4a, c). The absence of GAS-6 in *Axl*$^{-/-}$ spleens (Fig. 5a) was not due to an inability of *Axl*$^{-/-}$ splenic macrophages to express the *Gas6* gene, since we saw no difference in the *Gas6* mRNA in *Axl*$^{-/-}$ versus wild-type spleens (Fig. 5f). GAS-6 protein translation also occurs normally in TAM TKO BMDMs in culture (Fig. 1e). Finally, the ‘missing GAS-6’ of *Axl*$^{-/-}$ tissues did

not accumulate in the circulation, since the low concentration of GAS-6 normally present in serum was unchanged in *Axl*$^{-/-}$ mice (Fig. 5g). Together, these data indicate that maintenance of a GAS-6 protein reservoir in many tissues is dependent on the surface expression of Axl, and that in these tissues GAS-6 is normally pre-bound to Axl. We know of no equivalent dependence for other RTKs and their ligands.

Antibody-mediated TAM activation

RTKs are activated by ligand-driven dimerization and multimerization of receptor subunit monomers[31]. As such, antibodies generated against RTK ectodomains often act as ligand-independent RTK activators through their ability to drive receptor dimerization[32,33]. Although cross-activation of Mer has been described using a combination of primary and secondary antibodies[34], directly activating anti-TAM antibodies have not yet been reported. We found that affinity-purified, polyclonal anti-Axl (R&D, AF854), anti-Mer (R&D, AF591), and anti-TYRO3 (R&D, AF759) antibodies activated their respective receptors (Fig. 6a and data not shown). In contrast to GAS-6, which activates all three TAM receptors, the α-Mer and α-Axl antibodies displayed absolute receptor specificity (Fig. 6b).

We assessed the utility of these antibodies as TAM activators *in vivo*. We first injected the α-Axl antibody intravenously (IV), and monitored Axl and Mer activation and expression in the spleen. We found that splenic Axl was activated within 15 min after injection, and that its activity returned to baseline by 24 h (Fig. 6c). Mer was not activated by α-Axl, and control IgG had no effect on either Axl activation or expression (Fig. 6c). As observed previously[35,36], we found that strong Axl activation led to the rapid cleavage of the Axl ectodomain from the cell surface, a consequent loss of steady-state Axl, and the appearance of soluble Axl ectodomain (sAxl) (Fig. 6c).

We next measured the ability of varying doses of the antibodies to activate their receptors in liver, lung, and spleen. We detected dose-dependent activation of Axl in spleen and lung, again associated with splenic Axl cleavage, which was especially notable at the highest antibody dose (Fig. 6d). In liver, Axl cleavage was so robust that we were unable to detect any remaining Axl protein 1 h after injection of either 50 μg or 10 μg of the antibody (Fig. 6d). We also observed dose-dependent Mer activation in these tissues at 1 h after injection of the α-Mer antibody (Fig. 6e). Mer activation was strongest in liver and lung, and in contrast to Axl, was not associated with cleavage or loss of Mer protein (Fig. 6e). These results indicated that activating antibodies are specific tools for the activation of individual TAM receptors.

TAM activation alone is insufficient for phagocytosis

The TAM activating antibodies allowed us to test whether TAM activation in the absence of ligand could promote phagocytosis. We found that addition of either α-Axl or α-Mer activating antibody alone - in the absence of added GAS-6 – had zero stimulatory effect on apoptotic cell phagocytosis (Fig. 6f, g). Moreover, the addition of these receptor-activating antibodies in the presence of GAS-6 actually inhibited GAS-6-stimulated apoptotic cell phagocytosis (Fig. 6f, g). (This inhibition could result from antibody competition with GAS-6 for receptor binding or, for α-Axl, antibody-induced Axl cleavage.) Thus, TAM

activation is necessary for apoptotic cell phagocytosis by macrophages (Fig. 4d), but activation in the absence of a tripartite receptor-ligand-apoptotic cell (PtdSer) bridging interaction[8] is not sufficient for phagocytosis.

Axl activation inhibits inflammatory responses *in vivo*

Since Axl activation in DCs inhibits type I IFN production and signaling[5], we hypothesized that treatment with the α-Axl activating antibody, even though it does not promote phagocytosis, might be anti-inflammatory *in vivo*. To test this possibility, we injected mice IP with LPS (or saline as a control) concomitantly with either the activating α-Axl antibody or with control IgG, and then measured the type I IFN mRNAs in the spleen 2 h after injection. We observed a marked suppression of *Ifnb* and *Ifna4* mRNAs in mice injected with the α-Axl antibody, but not control IgG (Fig. 6h, i). These results suggest that activating α-Axl antibodies represent a viable approach to TAM-specific immunosuppressive therapeutics.

Overall, our results demonstrate that Axl and Mer are operationally distinct receptors. They reveal a pronounced diversification of TAM receptor expression, activity, function, ligand utilization, and proteolytic processing – as summarized in Supplementary Fig. 8.

DISCUSSION

Axl and Mer segregate into distinct niches of expression and function: Mer acts primarily in settings of steady state and induced tolerance, whereas Axl is specialized to act in the feedback inhibition of inflammation. Inflammatory stimuli that elevate Axl expression tend to depress Mer, and immunosuppressive stimuli that elevate Mer tend to depress Axl. Axl is induced in both M1- and M2-polarized macrophages, suggesting that it is a response receptor to nearly any inflammatory insult or tissue injury. Both Axl and Mer function as immunosuppressive phagocytic receptors, but they operate in inflammatory and tolerogenic environments, respectively.

When activated by ligand binding, Axl promotes the cleavage of its extracellular domain from the cell surface through the activation of proteases[35,36]. We found that this cleavage, which generates a ‘soluble Axl’ (sAxl), also occurred when Axl was activated by cross-linking antibodies. Elevated sAxl in blood has recently been reported to mark multiple human disease and trauma states, including aortic aneurysm[37], lupus flares[38], pneumonia infection[39], preeclampsia[40], coronary bypass[41], and insulin resistance[42]. We suggest that Axl cleavage, and the generation of a sAxl-GAS-6 complex, is triggered by the inflammation-induced exposure of PtdSer in these settings, and may be a broadly useful diagnostic biomarker for inflammation in human disease.

Although Mer also acts to suppress inflammation[43,44], it does so in two settings that are very different from the inflammatory environment in which Axl operates. The first is in normal tissues that are subject to continuous cellular renewal throughout life, and in which billions of apoptotic cells are generated and cleared on a regular, often circadian, schedule[45,46]. The second is during enhanced immune tolerance induced by corticosteroids and LXR agonists [19,20]. We show that the ability of these agents to stimulate phagocytosis of

apoptotic cells is entirely dependent on their ability to upregulate macrophage expression of Mer.

Our data indicate that Mer versus Axl polarization in homeostatic versus inflammatory settings, respectively, extends to multiple other phagocytic mediators, and suggests that distinct subgroups of phagocytic receptors are specialized to orchestrate apoptotic cell clearance in different environments. Axl cleavage upon activation suggests that Axl may be required only for initial stages of apoptotic cell phagocytosis. This is in agreement with recent work suggesting that Axl is a tethering receptor for apoptotic cells and that it co-operates with LRP-1 for engulfment[18]. Consistent with this suggestion, we observed that LRP1 (CD91) is co-regulated with Axl by Dex.

The segregation of Axl and Mer extends to their ligands. Unlike the other TAMs, Axl and GAS-6 are co-dependent: Axl uniquely depends on GAS-6 for its activation and GAS-6 requires Axl for its stable maintenance *in vivo*. The constitutive presence of an Axl-GAS-6 complex in tissues suggests that exposure of PtdSer may be the actual trigger for Axl activation. Indeed, the low basal activity of Axl complexed with GAS-6 is significantly enhanced by exposure to PtdSer-rich membranes.

Their divergence notwithstanding, both Axl and Mer mediate the PtdSer-dependent phagocytosis of apoptotic cells, and our results illuminate several features of the bridging model for this process[3,8]. In this model, GAS-6 or Protein S binds concommitantly a TAM receptor on the phagocyte surface and PtdSer on the apoptotic cell. First, we showed that activation of TAM kinase activity is necessary for phagocytosis, indicating that TAM receptors serve as more than passive apoptotic cell docking sites on the surface of phagocytes. Second, we showed that TAM kinase activation is not sufficient for apoptotic cell phagocytosis. And third, we observed rapid mobilization of the receptors to sites of apoptotic cell contact upon addition of purified ligands. Thus, TAM ligand interpolation between the macrophage and its phagocytic target is obligatory.

Finally, TAM receptor divergence is relevant to human therapy. TAM inhibitors are in development for cancer therapies[13,47,48] and treatment of enveloped virus infections[10]. Conversely, TAM activators have been proposed as treatments for autoimmune indications[49,50]. The fact that Mer functions on a daily basis throughout decades of adult life suggests that its long-term inhibition in the course of a cancer therapy should be evaluated for the development of impaired vision, reduced male fertility, and autoimmune disease as side effects. Long-term inhibition of Axl may result in fewer adverse reactions. In several settings, antibody-based therapies may have the advantage of absolute receptor specificity. Importantly, the finding that Axl downregulation is brought about through ectodomain cleavage calls into question the utility of Axl activation as a vehicle for cytotoxic drug delivery in Axl-overexpressing tumors. At the same time, the use of activating anti-Axl antibodies - for example, in the potential treatment of lupus or arthritis flares - should have the advantage of being self-limiting due to this receptor cleavage. Our results indicate that such antibodies may also be effective in the control of inflammation subsequent to infection. These and related considerations suggest that TAM modulation is an especially promising approach to the treatment of human disease.

ONLINE METHODS

Mice

The *Tyro3*$^{-/-}$, *Axl*$^{-/-}$, and *Mertk*$^{-/-}$ strains[9] and the *Gas6*$^{-/-}$ strain[51] were as described previously. All lines, except for the TAM TKOs, have been backcrossed for >9 generations to a C57BL/6 background. All animal procedures were conducted according to guidelines established by the Salk Institutional Animal Care and Use Committee. Mice (8–12-weeks old, both males and females) were randomly allocated to experimental groups and group allocation was not recognized during the experiment. Group size was based on previous literature.

Reagents and antibodies

Dexamethasone, hydrocortisone, cortisone, aldosterone, 17β-estradiol, estrone, estriol, progesterone, DMSO, and β-1,3-glucan from *Euglena gracilis* were from Sigma-Aldrich. Cell Tracker Orange (CMRA) was from Life Technologies. Pam3CSK4, HKLM, poly(I:C), LPS from *Escherichia coli*, ST-FLA, FSL-1, gardiquimod, CpG, MDP, iE-DAP, ppp-dsRNA-Lyo vector were from Invivogen. LPS from *Salmonella Minnesota* R595 was from List Biological Laboratories. LPS for *in vivo* use was from *E. coli* serotype O55:B5 (Enzo). Mouse cytokines were IL-4 (Cell Signaling), TNF (Cell Signaling), IFN-α11 (PBL), IFN-β (PBL), IFN-γ (BioVision). Purified human Protein S was from Haematologic Technologies Inc. T0901317, GW501516, BRL49653 were kindly provided by Ron Evans, Salk Institute. BMS-777607 was from Selleck Chemicals. Recombinant mouse GAS-6 was produced as described previously[10].

Antibodies used were: Mer (R&D, AF591), Axl (R&D, AF854), Axl for immunoprecipitation (Santa Cruz, M-20), TYRO3 (Santa Cruz, C-20, sc-1095), GAPDH (Millipore, MAB374, clone 6C5), phospho-tyrosine (Millipore, clone 4G10), GAS-6 (R&D, AF986), Protein S (R&D, AF4036), p-NF-κB p65 (Cell Signaling, 3033, clone 93H1), NF-κB (Cell Signaling, 4764, clone C22B4), STAT1 (Cell Signaling, 9172), Akt (Cell Signaling, 4691, clone C67E7), p-Akt (Cell Signaling, 4058, clone 193H12), Erk1/2 (Cell Signaling, 4695, clone 137F5), p-Erk1/2 (Cell Signaling, 9101), p38 (Cell Signaling, 8690, clone D13E1) and p-p38 (Cell Signaling, 4511, clone D3F9). Axl, Mer, TYRO3 and GAS-6 antibody specificity for immunohistochemistry, immunocytochemistry, immunoprecipitation and immunoblotting was tested using samples from respective genetically deficient animals (for example Fig. 1a, 5g and Supplementary Fig. 2b,c).

BMDM and BMDC cultures

Bone marrow cell cultures were differentiated as previously described for BMDMs[52] and BMDCs[16]. Briefly, tibias and femurs from 6–8-week-old mice were flushed with sterile DPBS (Mediatech), and red blood cells were lysed with ACK lysis buffer (Lonza). For BMDMs, bone marrow cells were plated on Petri dishes in DMEM (Mediatech) supplemented with 10% FBS (SAFC Biosciences), PenStrep and 20% L929 supernatant. Fresh differentiation media was added on day 4. On day 7, macrophages were washed once with DPBS and split by scraping with a cell scraper. Cells were plated in DMEM with 10% FBS to allow adhesion. Once the cells attached, the media was changed to fresh serum-free

media prior to experiments. For BMDCs, bone marrow cells were plated on 6-well plates in RPMI (Mediatech) supplemented with 5% FBS, 20 ng/ml mouse GM-CSF (Akron Biotech) and antibiotic-antimycotic cocktail (Invitrogen). Fresh differentiation media was added on day 4. On day 7, DC aggregates were dislodged by gently pipetting over the adherent stroma. Dislodged cells were pooled and resuspended in serum-free RPMI before experiments.

Cell stimulation with TAM ligands and activating antibodies

For TAM receptor activation BMDM or BMDC cultures were incubated with serum-free medium for 18 h with or without addition of the indicated stimuli. Cells were then stimulated with indicated concentration of recombinant mouse GAS-6, purified human Protein S or activating antibodies for the indicated time (10–30 min), and then lysed for protein isolation.

Immunoblotting and Immunoprecipitation

BMDM and BMDC cultures were washed with ice-cold DPBS and lysed on ice in a buffer containing 50 mM Tris-HCl pH 7.5, 1 mM EGTA, 1 mM EDTA, 1% Triton X-100, 0.27 M sucrose, 0.1% β-mercaptoethanol, and protease and phosphatase inhibitors (Roche). Tissues were snap frozen in liquid nitrogen prior to lysis. For immunoblots, equal amounts of protein (10 μg) in LDS sample buffer (Invitrogen) were subjected to electrophoresis on 4–12% Bis-Tris polyacrylamide gels (Novex, Life Technologies) and transferred to PVDF membranes (Millipore). For immunopreciptations, cell lysates were incubated overnight (ON) at 4°C with indicated antibodies. Protein G-Sepharose (Invitrogen) was added for 2 h and immunoprecipitates (IPs) were washed twice with 1 ml of lysis buffer containing 0.5 M NaCl and once with 1 ml of 50 mM Tris-HCl pH 7.5. IPs were eluted in LDS buffer, separated on polyacrylamide gels and transferred to PVDF membranes. Membranes were blocked in TBST (50 mM Tris-HCl pH 7.5, 0.15 M NaCl, and 0.25% Tween-20) containing 5% BSA and immunoblotted ON at 4°C with primary antibodies diluted 1000-fold in blocking buffer. Blots were then washed in TBST and incubated for 1 h at 22–24°C with secondary HRP-conjugated antibodies (GE Healthcare) diluted 5000-fold in 5% skim milk in TBST. After repeating the washes, signal was detected with enhanced chemiluminescence reagent.

ELISA

ELISAs for measurement of TNF (eBiosciences) and GAS-6 (R&D) were performed according to manufacturers' instructions.

Surface biotinylation

Cell surface biotinylation was performed as described[53]. Briefly, cells were washed three times with ice-cold PBS pH 8.0 and incubated for 30 min at 4°C with 1 mg/ml Sulfo-NHS-LC-Biotin (Thermo) in PBS pH 8.0. Cells were then washed three times with ice-cold 100 mM glycine in PBS and lysed.

Immunocytochemistry and immunohistochemistry

For immunohistochemistry tissues were fresh frozen and cut into 11 μm sections, air-dried and stored desiccated at −70°C. Prior to staining sections were fixed for 3 min with ice-cold acetone, washed in PBS, blocked in blocking buffer (PBS containing 0.1% Tween-20, 5% donkey serum and 2% IgG-free BSA) for 1 h. Slides were then washed in PBS 0.1% Tween-20 and incubated with 1 μg/ml primary antibody in blocking buffer ON at 4°C. Slides were then washed five times 5 min in PBS 0.1% Tween-20 and incubated with Hoechst and fluorophore-coupled donkey (Jackson) secondary antibodies diluted 1:400 in blocking buffer for 2 h at 22–24°C in dark. Slides were washed, sealed with Fluoromount-G (SouthernBiotech) and stored at 4°C. For immunocytochemistry cells were plated on cover slips and treated with indicated stimuli. For fixed labeling cells were first fixed in 4% PFA for 10 min and washed with PBS. Cover slips were then blocked for 30 min in blocking buffer with 0.1% Triton X-100, washed in PBS 0.1% Tween-20 and incubated with primary antibody for 1 h at 22–24°C. Cover slips were washed five times in PBS 0.1% Tween-20 and incubated with Hoechst and fluorophore-coupled donkey secondary antibody diluted 1:400 in blocking buffer for 1 h at 22–24°C in dark. Cover slips were washed and mounted on slides with Fluoromount-G. For live labeling, cells were incubated for 30 min at 4°C with primary antibody diluted to 1 μg/ml in cold media. Cells were washed three times with cold DPBS and fixed for 10 min with 4% PFA. Cover slips were blocked, incubated with secondary antibodies, washed and mounted as above. Images were taken on a Zeiss LSM 710 microscope with Plan-Apochromat 20x/0.8 M27 and 63x/1.40 Oil DIC M27 objectives at the Salk Waitt Advanced Biophotonics Center Core (WABC) Facility.

Scanning electron microscopy

Cells on coverslips were fixed in 3% glutaraldehyde and 3% paraformaldehyde in PBS pH 7.5 at 4°C overnight. The samples were then dehydrated in a graded ethanol series on ice. After dehydration, the coverslips were loaded into Teflon sample holders and processed in an automated critical point drier (Leica EM CPD300, Leica), which was set to perform 25 exchange cycles of CO_2 at medium speed and 20% stirring. All additional fill, heating, and venting steps were performed at medium speed as well. After drying, the coverslips were carefully removed and adhered to double-sided carbon tabs on aluminum stubs. The mounted samples were then sputter coated (Leica SCD500, Leica) with approximately 7 nm of platinum while being rotated. The samples were then imaged on an SEM (EVO HD, Zeiss Ltd.) at 3kV for optimal contrast. The entire procedure was performed at the WABC Facility, Salk Institute.

RT-qPCR

Total cellular RNA was isolated using RNeasy Mini Kit (Qiagen) according to manufacturer’s instructions. DNA was removed by on-column DNase (Qiagen) digest. Reverse transcription was performed with RT Transcriptor First Strand cDNA Synthesis Kit (Roche) with anchored oligo-dT primers (Roche). qPCR was run in a 384-well plate format on a ViiA 7 Real-Time PCR System (Applied Biosystems) using 2x SYBR Green PCR Master Mix (Applied Biosystems). Analysis was done using delta Ct method. Primers are listed in Supplementary Table 1.

Phagocytosis assay

Differentiated BMDMs were plated on a 48-well plate at 70% confluency and incubated for 24 h in DMEM containing indicated stimuli. To generate apoptotic cells, thymocytes were isolated from 3–6 week old mice, red blood cells were lysed with ACK buffer and remaining cells were incubated for 6 h in RPMI containing 5% FCS and 2 μM Dex to induce apoptosis. This routinely resulted in 70% apoptotic and ≤5% necrotic cells. Apoptotic cells were then stained with 100 ng/ml pHrodo-SE (Invitrogen) for 30 min as previously described[27]. Labeled cells were washed twice in PBS containing 1% BSA (to block remaining pHrodo-SE) and 1 mM EDTA (to remove any bound GAS-6 and Protein S) and once with DMEM. Apoptotic cells were then incubated for 10 min with indicated concentration of recombinant mouse GAS-6 or purified human Protein S and added to macrophages at the ratio 10:1 (apoptotic cells:phagocyte) and incubated for 1 h at 37°C. BMDMs were then briefly washed in DPBS and incubated in trypsin (0.25%) for 10 min at 37°C, placed on ice, and detached by vigorous pipetting. Phagocytosis was assessed by flow cytometry with post-acquisition data analysis using FlowJo software (Treestar). pHrodo fluorescence was measured with excitation at 561 nm and emission filters for PE (574–590 nm) on LSRII (BD Biosciences) at the Flow Cytometry Core, Salk Institute. For *in vivo* phagocytosis assay, pHrodo-labeled apoptotic cells were injected intraperitoneally. After 1 h peritoneal cavity was washed with ice cold PBS and the percent of $CD11b^+$ $pHrodo^+$ phagocytic macrophages was quantified by flow cytometry.

Activating antibodies *in vivo*

Male 8–12-week-old mice were injected IV (retro-orbital injection, 0.2 ml final volume) or IP (0.3 ml final volume) with α-Axl (R&D, AF854) and α-Mer (R&D, AF591) activating antibodies or control IgG (R&D, AB-108-C) at indicated concentration. Mice were sacrificed at specified time points post injection and tissues were snap frozen in liquid nitrogen for further analysis of protein and mRNA.

Data analysis

All experiments were performed in duplicates or triplicates and repeated at least 3 times. Replicate number was chosen to be adequate for the statistical method used. Data had normal distribution and equal variance, and are shown as means ± s.d. from multiple independent experiments or mice. Statistical analysis was performed using two-tailed Student's *t*-test.

Supplementary Material

Refer to Web version on PubMed Central for supplementary material.

Acknowledgments

We thank M. Joens and J. Fitzpatrick (WABC Facility, Salk Institute) for processing samples and acquiring SEM images, R. Evans (Salk Institute) for sharing nuclear receptor agonists, J. Hash, P. Burrola, and C. Mayer for excellent technical support, and members of the Lemke lab and the Nomis Center for helpful discussions. This research was supported by grants from the National Institutes of Health (R01 AI077058, R01 AI101400, and R01 NS085296 to G.L.) and the Leona M. and Harry B. Helmsley Charitable Trust (to G.L.), by the Nomis, H. N. and Frances C. Berger, Fritz B. Burns, and HKT Foundations, by Françoise Gilot-Salk, and by postdoctoral fellowships

from the Human Frontiers Science Program (to A.Z.), the Marie Curie International Outgoing Fellowships (to P.G.T.), and the Leukemia and Lymphoma Society and the Nomis Foundation (to E.D.L.).

References

1. Munoz LE, Lauber K, Schiller M, Manfredi AA, Herrmann M. The role of defective clearance of apoptotic cells in systemic autoimmunity. Nat Rev Rheumatol. 2010; 6:280–289. [PubMed: 20431553]
2. Lemke G. Biology of the TAM receptors. Cold Spring Harbor Perspectives. 2013; 5(11)10.1101/cshperspect.a009076
3. Lemke G, Rothlin CV. Immunobiology of the TAM receptors. Nat Rev Immunol. 2008; 8:327–336. [PubMed: 18421305]
4. Lu Q, Lemke G. Homeostatic regulation of the immune system by receptor tyrosine kinases of the Tyro 3 family. Science. 2001; 293:306–311. [PubMed: 11452127]
5. Rothlin CV, Ghosh S, Zuniga EI, Oldstone MB, Lemke G. TAM receptors are pleiotropic inhibitors of the innate immune response. Cell. 2007; 131:1124–1136. [PubMed: 18083102]
6. Burstyn-Cohen T, et al. Genetic dissection of TAM receptor-ligand interaction in retinal pigment epithelial cell phagocytosis. Neuron. 2012; 76:1123–1132. [PubMed: 23259948]
7. Scott RS, et al. Phagocytosis and clearance of apoptotic cells is mediated by MER. Nature. 2001; 411:207–211. [PubMed: 11346799]
8. Lemke G, Burstyn-Cohen T. TAM receptors and the clearance of apoptotic cells. Ann N Y Acad Sci. 2010; 1209:23–29. [PubMed: 20958312]
9. Lu Q, et al. Tyro-3 family receptors are essential regulators of mammalian spermatogenesis. Nature. 1999; 398:723–728. [PubMed: 10227296]
10. Bhattacharyya S, et al. Enveloped Viruses Disable Innate Immune Responses in Dendritic Cells by Direct Activation of TAM Receptors. Cell Host Microbe. 2013; 14:136–147. [PubMed: 23954153]
11. Meertens L, et al. TIM and TAM receptors mediate dengue virus infection. Cell Host and Microbe. 2012; 12:544–557. [PubMed: 23084921]
12. Paolino M, et al. Essential role of E3 ubiquitin ligase activity in Cbl-b-regulated T cell functions. J Immunol. 2014; 186:2138–2147. [PubMed: 21248250]
13. Schlegel J, et al. MERTK receptor tyrosine kinase is a therapeutic target in melanoma. J Clin Invest. 2013; 123:2257–2267. [PubMed: 23585477]
14. Meyer AS, Miller MA, Gertler FB, Lauffenburger DA. The receptor AXL diversifies EGFR signaling and limits the response to EGFR-targeted inhibitors in triple-negative breast cancer cells. Sci Signal. 2013; 6:ra66. [PubMed: 23921085]
15. Carrera Silva EA, et al. T cell-derived protein S engages TAM receptor signaling in dendritic cells to control the magnitude of the immune response. Immunity. 2013; 39:160–170. [PubMed: 23850380]
16. Inaba K, et al. Isolation of dendritic cells. Curr Protoc Immunol. 2009; Chapter 3(Unit 3):7. [PubMed: 19653207]
17. Rahman ZS, Shao WH, Khan TN, Zhen Y, Cohen PL. Impaired apoptotic cell clearance in the germinal center by Mer-deficient tingible body macrophages leads to enhanced antibody-forming cell and germinal center responses. J Immunol. 2010; 185:5859–5868. [PubMed: 20952679]
18. Subramanian M, et al. An AXL/LRP-1/RANBP9 complex mediates DC efferocytosis and antigen cross-presentation in vivo. J Clin Invest. 2014
19. McColl A, et al. Glucocorticoids induce protein S-dependent phagocytosis of apoptotic neutrophils by human macrophages. J Immunol. 2009; 183:2167–2175. [PubMed: 19597001]
20. A-Gonzalez N, et al. Apoptotic cells promote their own clearance and immune tolerance through activation of the nuclear receptor LXR. Immunity. 2009; 31:245–258. [PubMed: 19646905]
21. Mukundan L, et al. PPAR-delta senses and orchestrates clearance of apoptotic cells to promote tolerance. Nat Med. 2009; 15:1266–1272. [PubMed: 19838202]
22. Clark AR. Anti-inflammatory functions of glucocorticoid-induced genes. Mol Cell Endocrinol. 2007; 275:79–97. [PubMed: 17561338]

23. Mosser DM, Edwards JP. Exploring the full spectrum of macrophage activation. Nat Rev Immunol. 2008; 8:958–969. [PubMed: 19029990]
24. Feng X, et al. Lipopolysaccharide inhibits macrophage phagocytosis of apoptotic neutrophils by regulating the production of tumour necrosis factor alpha and growth arrest-specific gene 6. Immunology. 2011; 132:287–295. [PubMed: 21039473]
25. Nishi C, Toda S, Segawa K, Nagata S. Tim4- and MerTK- mediated engulfment of apoptotic cells by mouse resident peritoneal macrophages. Mol Cell Biol. 2014; 34:1512–1520. [PubMed: 24515440]
26. Seitz HM, Camenisch TD, Lemke G, Earp HS, Matsushima GK. Macrophages and dendritic cells use different Axl/Mertk/Tyro3 receptors in clearance of apoptotic cells. J Immunol. 2007; 178:5635–5642. [PubMed: 17442946]
27. Miksa M, Komura H, Wu R, Shah KG, Wang P. A novel method to determine the engulfment of apoptotic cells by macrophages using pHrodo succinimidyl ester. J Immunol Methods. 2009; 342:71–77. [PubMed: 19135446]
28. Oka K, et al. Lectin-like oxidized low-density lipoprotein receptor 1 mediates phagocytosis of aged/apoptotic cells in endothelial cells. Proc Natl Acad Sci U S A. 1998; 95:9535–9540. [PubMed: 9689115]
29. Park D, et al. BAI1 is an engulfment receptor for apoptotic cells upstream of the ELMO/Dock180/Rac module. Nature. 2007; 450:430–434. [PubMed: 17960134]
30. Schroeder GM, et al. Discovery of N-(4-(2-amino-3-chloropyridin-4-yloxy)-3-fluorophenyl)-4-ethoxy-1-(4-fluorophenyl)-2-oxo-1,2-dihydropyridine-3-carboxamide (BMS-777607), a selective and orally efficacious inhibitor of the Met kinase superfamily. J Med Chem. 2009; 52:1251–1254. [PubMed: 19260711]
31. Lemmon MA, Schlessinger J. Cell signaling by receptor tyrosine kinases. Cell. 2010; 141:1117–1134. [PubMed: 20602996]
32. Kahn CR, Baird KL, Jarrett DB, Flier JS. Direct demonstration that receptor crosslinking or aggregation is important in insulin action. Proc Natl Acad Sci U S A. 1978; 75:4209–4213. [PubMed: 279910]
33. Schreiber AB, Libermann TA, Lax I, Yarden Y, Schlessinger J. Biological role of epidermal growth factor-receptor clustering. Investigation with monoclonal anti-receptor antibodies. J Biol Chem. 1983; 258:846–853. [PubMed: 6296087]
34. Todt JC, Hu B, Curtis JL. The receptor tyrosine kinase MerTK activates phospholipase C gamma2 during recognition of apoptotic thymocytes by murine macrophages. J Leukoc Biol. 2004; 75:705–713. [PubMed: 14704368]
35. O'Bryan JP, Fridell YW, Koski R, Varnum B, Liu ET. The transforming receptor tyrosine kinase, Axl, is post-translationally regulated by proteolytic cleavage. J Biol Chem. 1995; 270:551–557. [PubMed: 7822279]
36. Costa M, Bellosta P, Basilico C. Cleavage and release of a soluble form of the receptor tyrosine kinase ARK in vitro and in vivo. J Cell Physiol. 1996; 168:737–744. [PubMed: 8816929]
37. Ekman C, Site DF, Gottsater A, Lindblad B, Dahlback B. Plasma concentrations of growth arrest specific protein 6 and the soluble form of its tyrosine kinase receptor Axl as markers of large abdominal aortic aneurysms. Clin Biochem. 2010; 43:110–114. [PubMed: 19660445]
38. Zhu H, et al. Different expression patterns and clinical significance of mAxl and sAxl in systemic lupus erythematosus. Lupus. 2014; 23:624–634. [PubMed: 24474706]
39. Ko CP, Yu YL, Hsiao PC, Yang SF, Yeh CB. Plasma levels of soluble Axl correlate with severity of community-acquired pneumonia. Mol Med Rep. 2014; 9:1400–1404. [PubMed: 24503651]
40. Liu X, et al. Plasma concentrations of sAxl are associated with severe preeclampsia. Clin Biochem. 2014; 47:173–176. [PubMed: 24239956]
41. Lee CH, et al. Plasma concentrations predict aortic expression of growth-arrest-specific protein 6 in patients undergoing coronary artery bypass grafting. PLoS One. 2013; 8:e79452. [PubMed: 24236135]
42. Hsiao FC, et al. Circulating growth arrest-specific 6 protein is associated with adiposity, systemic inflammation, and insulin resistance among overweight and obese adolescents. J Clin Endocrinol Metab. 2013; 98:E267–274. [PubMed: 23341490]

43. Camenisch TD, Koller BH, Earp HS, Matsushima GK. A novel receptor tyrosine kinase, Mer, inhibits TNF-alpha production and lipopolysaccharide-induced endotoxic shock. J Immunol. 1999; 162:3498–3503. [PubMed: 10092806]
44. Sen P, et al. Apoptotic cells induce Mer tyrosine kinase-dependent blockade of NF-kappaB activation in dendritic cells. Blood. 2007; 109:653–660. [PubMed: 17008547]
45. Casanova-Acebes M, et al. Rhythmic modulation of the hematopoietic niche through neutrophil clearance. Cell. 2013; 153:1025–1035. [PubMed: 23706740]
46. Scheiermann C, Kunisaki Y, Frenette PS. Circadian control of the immune system. Nat Rev Immunol. 2013; 13:190–198. [PubMed: 23391992]
47. Holland SJ, et al. R428, a selective small molecule inhibitor of Axl kinase, blocks tumor spread and prolongs survival in models of metastatic breast cancer. Cancer Res. 2010; 70:1544–1554. [PubMed: 20145120]
48. Ye X, et al. An anti-Axl monoclonal antibody attenuates xenograft tumor growth and enhances the effect of multiple anticancer therapies. Oncogene. 2010; 29:5254–5264. [PubMed: 20603615]
49. Rothlin CV, Lemke G. TAM receptor signaling and autoimmune disease. Curr Opin Immunol. 2010; 22:740–746. [PubMed: 21030229]
50. van den Brand BT, et al. Therapeutic efficacy of Tyro3, Axl, and Mer tyrosine kinase agonists in collagen-induced arthritis. Arthritis Rheum. 2013; 65:671–680. [PubMed: 23203851]
51. Angelillo-Scherrer A, et al. Deficiency or inhibition of Gas6 causes platelet dysfunction and protects mice against thrombosis. Nat Med. 2001; 7:215–221. [PubMed: 11175853]
52. Zhang X, Goncalves R, Mosser DM. The isolation and characterization of murine macrophages. Curr Protoc Immunol. 2008; Chapter 14(Unit 14):11.
53. Fourgeaud L, et al. The metabotropic glutamate receptor mGluR5 is endocytosed by a clathrin-independent pathway. J Biol Chem. 2003; 278:12222–12230. [PubMed: 12529370]

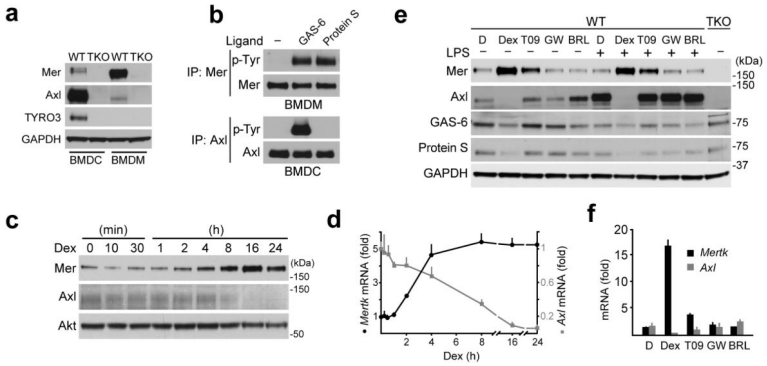

Fig. 1. Differential expression and activation of Axl and Mer

(**a**) Immunoblot showing TAM receptor expression and antibody specificity in BMDC and BMDM cultures from WT and TAM TKO mice. The exposure of the Axl and Mer immunoblots in this panel is longer than in subsequent figures to visualize the very low expression of Mer in BMDCs and Axl in BMDMs. Representative of two independent experiments. *Axl* mRNA copy number (per ng of total RNA ± s.d.) was 29±4 and 28±9 in BMDC and BMDM cultures, respectively, suggesting that most of the difference between these cells is post-transcriptional; whereas for *Mer* mRNA, these numbers were 3±1 and 37±6 in BMDC and BMDM cultures, respectively.

(**b**) BMDM and BMDC cultures were stimulated with 10 nM GAS-6 or 25 nM Protein S for 10 min and receptor activation was assayed by immunoprecipitation and immunoblotting. Representative of three independent experiments.

(**c**,**d**) Time course of Mer and Axl protein (**c**) and mRNA (**d**) in BMDM cultures upon 0.1 μM Dex stimulation assayed by immunoblotting (**c**) or RT-qPCR (**d**). (**c**) – representative of two independent experiments; (**d**) – fold of change normalized to *Hprt* mRNA. Average of two independent experiments, each done in technical duplicates, graphed as mean ± s.d.

(**e**,**f**) Expression of Mer and Axl protein (**e** - immunoblot) and mRNA (**f** - RT-qPCR) in BMDM cultures upon 24 h stimulation with nuclear receptor agonists: DMSO (D), 1 μM Dex (Dex), 1 μM T0901317 (T09), 0.2 μM GW501516 (GW), or 1 μM BRL49653 (BRL). 30 ng/ml LPS was added where indicated 8 h before lysis. (**e**) – representative of two independent experiments; (**f**) – fold of change relative to *Hprt* mRNA. Average of two independent experiments, each done in technical duplicates, graphed as mean ± s.d.

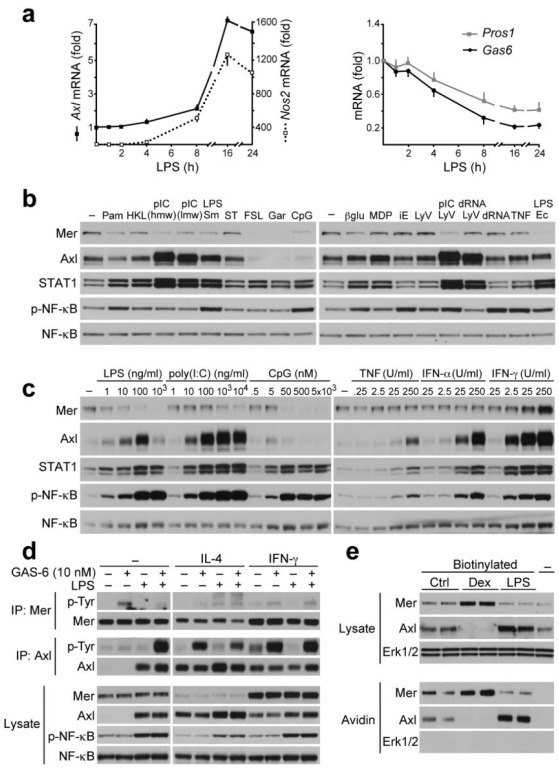

Fig. 2. Axl and Mer expression in inflammatory macrophages

(**a**) Time course of *Axl*, *Nos2*, *Gas6* and *Pros1* mRNA expression in BMDM cultures in response to 100 ng/ml LPS measured by RT-qPCR. There was virtually no basal expression of *Nos2* mRNA prior to stimulation. Data are presented as fold of change normalized to *Hprt* mRNA. Average of two independent experiments, each done in technical duplicates, graphed as mean ± s.d.

(**b**) Immunoblot showing Mer and Axl protein expression in cell lysates from BMDMs stimulated for 18 h with 100 ng/ml Pam3CSK4 (TLR1/2 ligand), 2×10^7 cells/ml HKLM (TLR2 ligand), 1 μg/ml poly(I:C) (pIC) high molecular weight (hmw) or low molecular weight (lmw) (TLR3 ligands), 100 ng/ml LPS from *Salmonella Minnesota* (TLR4 ligand), 100 ng/ml ST-FLA (TLR5 ligand), 100 ng/ml FSL-1 (TLR6/2 ligand), 1 μg/ml gardiquimod (TLR7 ligand), 0.5 μM CpG (ODN1826, TLR9 ligand), 1 μM β-glucan (Dectin ligand), 10 μg/ml MDP (NOD2 ligand), 10 μg/ml iE-DAP (NOD1 ligand), Lyo vector (control), 0.5 μg/ml ppp-dsRNA-Lyo vector (RIG-I ligand), 1 μg/ml pIC-Lyo vector (RIG-I and MDA5 ligand), 0.5 μg/ml ppp-dsRNA (control), TNF (25 U/ml), 100 ng/ml LPS from *Escherichia coli* (TLR4 ligand). STAT1 and pNF-κB (p65) used as activation markers and total NF-κB as lysate loading control here, and in (**c**) and (**d**). Representative of two independent experiments.

(**c**) Immunoblot showing Mer and Axl protein expression in BMDM stimulated for 18 h with indicated concentration of LPS, poly(I:C), CpG, TNF, IFN-α or IFN-γ. Representative of two independent experiments.

(**d**) BMDM cultures were treated for 18 h with 4 ng/ml IL-4 or 25 U/ml IFN-γ with or without 100 ng/ml LPS and then stimulated for 10 min with 10 nM GAS-6. Receptor

abundance and activation were monitored by receptor immunoprecipitation (IP) and anti-phosphotyrosine (p-Tyr) immunoblotting, as indicated. Representative of two independent experiments.

(**e**) BMDM cultures were treated for 18 h with 0.1 μM Dex or 100 ng/ml LPS and biotinylated prior to cell lysis. Axl and Mer presence on cell surface were analyzed in avidin pull downs. Representative of three independent experiments.

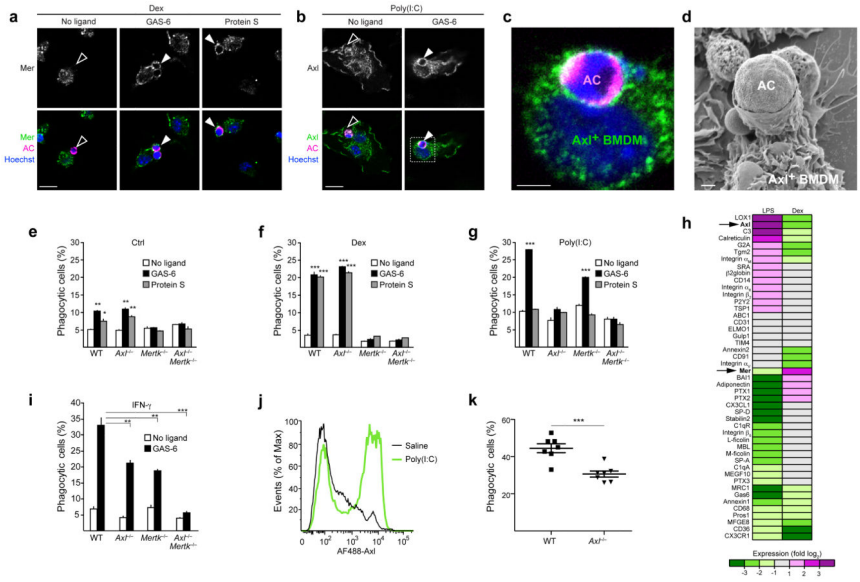

Fig. 3. Axl is a phagocytic receptor in activated macrophages

(**a**–**d**) BMDM cultures were treated with 0.1 μM Dex (**a**) or 10 μg/ml poly(I:C) (**b**–**d**) for 24 h and then fed with apoptotic cells (AC) stained with Cell Tracker Orange for 30 min in the presence or absence of the indicated TAM ligands. Cells were fixed and immunostained for Mer (**a**), Axl (**b**,**c**) or visualized by SEM (**d**). Open arrows: non-engulfed apoptotic cells attached to TAM-negative membrane; closed arrows: engulfed apoptotic cells surrounded by TAM-positive membrane; bars- 20 μm (**a** and **b**), 5 μm (**c**), 1 μm (**d**). Images are representative of n=10 images per each condition from two independent experiments.

(**e**–**g**,**i**) BMDM cultures derived from indicated knock-out mice were untreated (Ctrl) (**e**) or treated for 24 h with 0.1 μM Dex (**f**), 10 μg/ml poly(I:C) (**g**) or 250 U/ml IFN-γ (**i**) and then incubated for 1 h with pHrodo-labeled apoptotic cells with or without indicated TAM ligands. Percent of phagocytosis was measured using flow cytometry (see Online Methods). Data are presented as mean ± s.d. from two independent experiments, each done for duplicate cultures for each genotype and each condition. The statistical significance was analyzed by unpaired two-tailed *t*-test and is indicated for *p<0.05, **p<0.01 and ***p<0.001.

(**h**) BMDMs were untreated or treated for 24 h with 0.1 μM Dex or 100 ng/ml LPS. Expression of indicated genes was analyzed by RT-qPCR. For each transcript expression was normalized to *Cyclophilin A* mRNA and fold-change, relative to untreated cells, was calculated. Heat-map represents log2 of fold of change; average of 3 independent experiments. Statistical significance cutoff value for each gene was p<0.05, analyzed by two-tailed *t*-test.

(**j**) WT mice were injected intraperitoneally with saline or 100 μg poly(I:C). After 16 h peritoneal lavages were collected and Axl expression on $CD11b^+$ peritoneal macrophages was measured by flow cytometry. Plot is representative from n=3 mice for each condition.

(**k**) WT (n=7) or $Axl^{-/-}$ (n=7) mice were injected intraperitoneally with 100 μg poly(I:C). After 16 h mice were injected with pHrodo-labeled apoptotic cells for 1 h followed by the peritoneal lavage collection. Percent of phagocytic $CD11b^+$ macrophages was measured by flow cytometry. Each mouse is presented as a separate data point and mean ± s.e.m are

indicated. Data is pooled from two independent experiments. Statistical significance was analyzed by two-tailed *t*-test; p=0.0004.

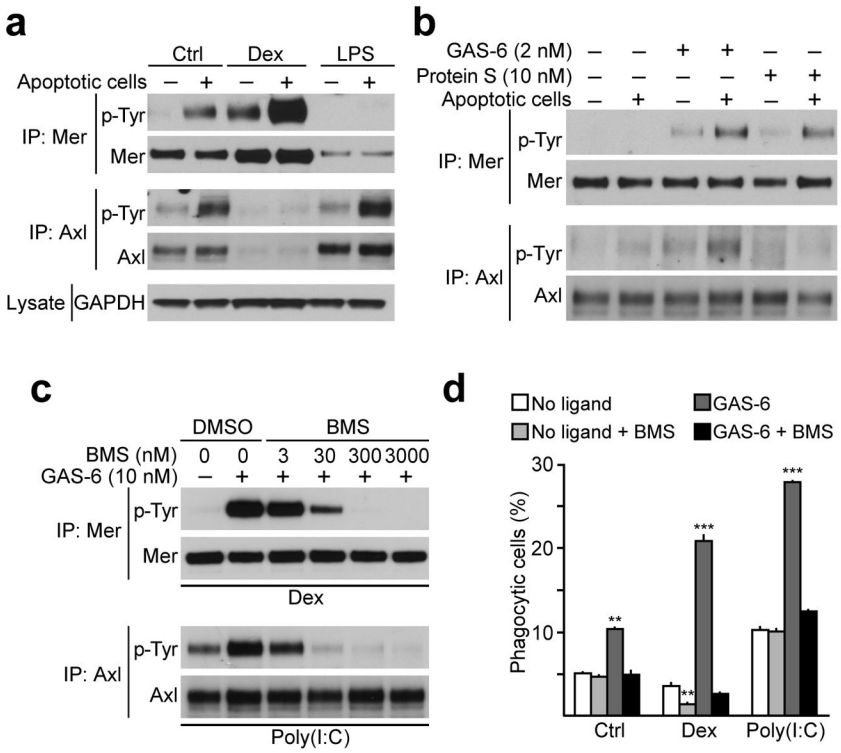

Fig. 4. Axl and Mer kinase activity is necessary for apoptotic cell phagocytosis

(**a**) BMDM cultures were stimulated for 18 h with 0.1 μM Dex or 100 ng/ml LPS and then incubated with apoptotic cells in 1:10 ratio for 30 min. Receptor activation was assayed by immunoprecipitation and anti-p-Tyr immunoblotting. Representative of two independent experiments.

(**b**) BMDM cultures were starved for 18 h, washed and then stimulated for 10 min with 2 nM GAS-6 or 10 nM Protein S with or without apoptotic cells. Representative of two independent experiments.

(**c**) BMDM cultures were cultured for 18 h with 0.1 μM Dex or 10 μg/ml poly(I:C), pretreated for 15 min with indicated concentration of BMS-777607 and then stimulated for 10 min with 10 nM GAS-6. Receptor activation assayed as in (**a**). Representative of two independent experiments.

(**d**) BMDM cultures were untreated or treated for 24 h with 0.1 μM Dex or 10 μg/ml poly(I:C) and then incubated for 1 h with pHrodo-labeled apoptotic cells with or without 10 nM GAS-6 and 300 nM BMS-777607 compound. Percent phagocytosis was measured using flow cytometry. Data are presented as mean ± s.d. from two independent experiments, each done for duplicate cultures for each condition. The statistical significance was analyzed by unpaired two-tailed *t*-test and is indicated for **p<0.01 and ***p<0.001.

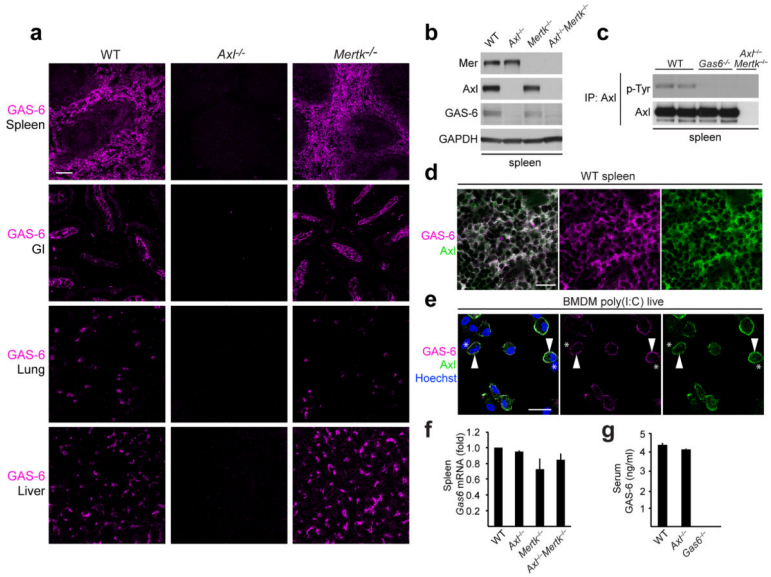

Fig. 5. GAS-6 is bound to Axl *in vivo* and *in vitro*

(**a**) GAS-6 immunohistochemistry in spleen, duodenum (GI), lung and liver sections from indicated mice. Bar, 100 μm. Representative sections from n=3 mice for each genotype.

(**b**) Immunoblot of Axl, Mer and GAS-6 protein in spleen extracts from indicated mice. Representative of two independent experiments.

(**c**) Basal Axl activation in spleen of indicated mice assayed by immunoprecipitation and immunoblotting. Each lane is a separate mouse. Representative of two independent experiments.

(**d**) Co-localization of Axl and GAS-6 in spleen red pulp. Bar, 20 μm. Representative sections from n=3 mice. $Axl^{-/-}$ and $Gas6^{-/-}$ mice were used to verify antibody specificity (not shown).

(**e**) Co-localization of Axl and GAS-6 on the surface of poly(I:C)-treated live BMDMs. Arrowheads: cells co-stained with Axl and GAS-6; asterisks: cells negative for both Axl and GAS-6. Bar, 20 μm. Representative of two independent experiments. Cells from $Axl^{-/-}$ and $Gas6^{-/-}$ mice were used to verify antibody specificity (not shown).

(**f**) RT-qPCR of *Gas6* mRNA in spleen from indicated mice. Average of n=2 mice for each genotype, normalized to *Actin* mRNA and graphed as mean fold of change ± s.d.

(**g**) GAS-6 protein in serum from indicated mice, measured by ELISA. Average of n=3 mice for each genotype graphed as mean ± s.d.

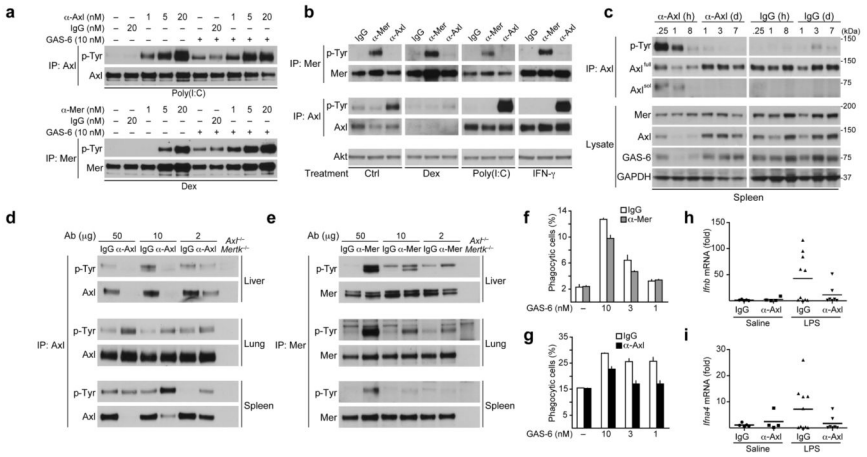

Fig. 6. Axl- and Mer-activating antibodies

(**a**) BMDM cultures were pre-treated with 0.1 μM Dex or 10 μg/ml poly(I:C) for 18 h, and then stimulated with control antibody, α-Axl or α-Mer activating antibody for 20 min, with or without addition of 10 nM GAS-6 for the final 10 min. Receptor activation was assayed by immunoprecipitation and immunoblotting. Representative of two independent experiments.

(**b**) BMDM cultures were pretreated for 18 h with 0.1 μM Dex, 10 μg/ml poly(I:C) or 250 U/ml IFN-γ and then stimulated for 10 min with 10 nM of the indicated activating antibody. Representative of two independent experiments.

(**c**) Mice were injected IV with 10 μg of α-Axl antibody or control IgG, and spleens were collected at the indicated time points. Axl receptor phosphorylation was assayed by immunoprecipitation and immunoblotting. GAS-6 presence was assayed by immunoblotting of total spleen lysates. Representative of two independent experiments.

(**d**,**e**) Mice were injected IV with indicated dose of α-Axl or control IgG (**d**) or α-Mer or control IgG (**e**) for 1 h. Axl and Mer receptor phosphorylation was assayed by immunoprecipitation and immunoblotting. Representative of two independent experiments.

(**f**,**g**) BMDM cultures were pretreated for 24 h with 0.1 μM Dex (**f**) or 10 μg/ml poly(I:C) (**g**) and the phagocytosis assay was performed in the presence of 10 nM α-Mer (**f**) or α-Axl (**g**) activating antibody and indicated concentrations of GAS-6. Data is presented as mean ± s.d. from two independent experiments, each done for duplicate cultures for each condition.

(**h**,**i**) WT mice were injected IP with saline or 10 μg LPS together with 10 μg of either control IgG or α-Axl activating antibody. *Ifnb* (**h**) and *Ifna4* (**i**) induction in spleen was measured by RT-qPCR relative to *Cyclophilin A* expression and presented as fold of change. Each mouse is plotted as a separate data point. Mean is indicated. n=5 (saline IgG), n=4 (saline α-Axl), n=10 (LPS IgG), n=7 (LPS α-Axl),